Available online at www.elixirpublishers.com (Elixir International Journal)

Thermal Engineering

Elixir Thermal Engineering 184 (2024) 57069 - 57078

ISSN: 2229-712X

Numerical and Experimental Analysis of the Operation of a Solar Adsorption Refrigerator under Sahelian Climatic Conditions: Case of Burkina Faso

Guy Christian Tubreoumya[1,2], Eloi Salmwendé Tiendrebeogo[1], Alfred Bayala[3], Téré Dabilgou[1,2], Belkacem Zeghmati[2], Alfa Oumar Dissa[1] and Antoine Bere[1]

[1]Laboratoire de Physique et de Chimie de l'Environnement (LPCE), Université Joseph Ki Zerbo, Ouagadougou, Burkina Faso.

[2]LAboratoire de Mathématiques et Physique (LA.M.P.S), Université de Perpignan Via Domitia (UPVD).

[3]Laboratoire d'Energies Thermiques Renouvelables, Ouagadougou Burkina Faso.

ARTICLE INFO

Article history:

Received: 11 November 2023;

Received in revised form:

15 December 2023;

Accepted: 15 February 2024;

Keywords

Solar Refrigeration,
Simulation,
Experimentation,
Adsorption,
Zeolite,
Water.

ABSTRACT

An experimental and numerical study of the operation of an adsorption solar refrigerator using the zeolite-water couple is presented. The experimental consists of measuring the solar radiation incident on the collector-absorber, the temperature of the collector-adsorber, of the condenser and the one of the evaporator. The numerical part concerns a modeling and a simulation of the functioning of this refrigeration system. Transfer equations are deduced from thermal and mass balances established at each component of the refrigerator. The Dubinin-Astakhov equation is adopted for the adsorption kinetics of the zeolite-water pair. The results are presented by the evolution over time of the temperatures of the components of the solar refrigerator (absorbent plate, condenser, evaporator, etc.), as well as the pressure adsorbed, adsorbate mass and SCOP.

1. Introduction

The adsorption solar refrigerator systems are quiet, adaptable to large or small medium. However, these systems are no longer competitive with compressor refrigeration systems which are very widespread. The operation of compressor refrigeration systems requires the use of refrigerants and consumption of electrical energy. These refrigerants, CFCs (chlorofluorocarbons), HCFCs (hydrochlorofluorocarbons) and HFCs (hydrofluorocarbons) are harmful to the ozone layer and contribute to increase the greenhouse effect. Since the Montreal Protocol in 1987 for the reduction of the use of these refrigerants [1], it seems that solar adsorption refrigeration machines represent a promising way to meet the environmental and energy concerns [2, 3, 4]. Indeed, the technology of these machines is simple. Its maintenance is easy and the materials used are recyclable [8]. In addition, they use refrigerants such as water [6, 7, 9, 10, 11], methanol [5, 12, 13, 14] and ammonia [15], which have no effect on the environment. The adsorption solar refrigerator systems seems to be an attractive application of solar energy in isolated regions where conventional electrical power is not available. Hence, in a country like Burkina Faso, in which the average solar irradiation varies between 5.5 $kWh.m^{-2}.day^{-1}$ and 6.5 $kWh.m^{-2}.day^{-1}$ [16], solar adsorption refrigeration is an adequate means to meet important needs such as food preservation, pharmaceuticals needs, air conditioning and consequently to the reduction of electricity consumption. However, the solar adsorption refrigerator presented several disadvantages such as, its low coefficient of performance, the weak heat and mass transfer in the adsorbent bed [17], the low thermal conductivity of the adsorbent [18, 19, 20], the poor contact adsorber-adsorbent [21, 22] and the discontinuous operation of the refrigeration cycle [23, 24]. Nonetheless various studies on the improvement of the performance of the solar adsorption refrigerator have been carried out. This improvement studies concern the use of vacuum tube collectors [12, 15, 25], the single glazed or double glazed flat plate collectors [26, 27, 28] and the cylindrical parabolic collectors [29, 30]. In addition, researches have focused on the way to improve the heat and mass transfer in the adsorbent bed. In these reseraches, the fins are commonly used. These fins act as thermal bridges between the absorbent plate and the reactive medium (adsorbent bed). This makes it possible to optimize heat and mass transfer in the adsorbent bed [17, 22, 31, 32, 33].

This paper aims at studying experimentally and numerically over a complete cycle, the effects of operation temperatures on a solar refrigeration systems under the climatic conditions of Burkina Faso.

2. Experimental study

2.1 Experimental setup

The experimental setup consists of three components: a collector-adsorber, a condenser, and a refrigerating enclosure containing the evaporator. These components are connected by a cylindrical and flexible tube of diameter 3 cm and length 240 cm. The adsorbent / adsorbate used is the zeolite / water couple. Figure 1 shows a photo of the experimental setup.

- **The collector-adsorber**: it is a parallelepipedic box of 1x1 m and height 20 cm. Its top wall is a glass cover of thickness 5 mm. The vertical and bottom walls made of aluminums are insulated by a 10 cm thick layer of glass wool. The adsorber contains the zeolite / water couple (20 kg of zeolite). The collector-adsorber assembly is inclined at an angle $\alpha = 13°$ to the horizontal
- **The condenser:** it consists of an aluminum tube of length 65 cm, thickness 5 mm and diameter 10 cm. It is provided with 52 fins spaced 1.5 cm apart. Each aluminum fin has a square shape of 20 cm side and 1 mm thick. The condenser exchange area is 7.5 m^2. The condenser is cooled by natural convection and is positioned so that the condensate flows towards the evaporator through one of the orifices under the effect of gravity towards the evaporator.
- **The evaporator:** it is located in a refrigerated enclosure. It is thermally insulated and dimensions 100x80x70 cm. It consists of an aluminum parallelepiped tank with fins and two tubes allowing the passage of water vapor during adsorption. The total exchange area of the evaporator is 0.7 m^2.

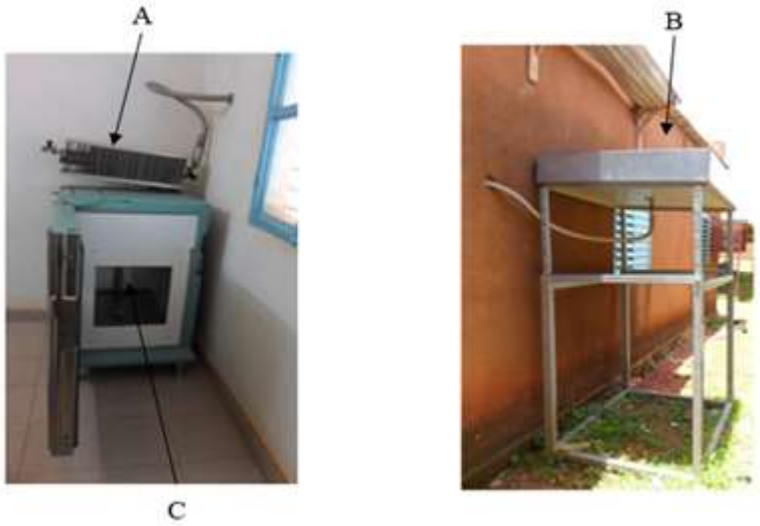

Figure 1. Photography of solar adsorption refrigerator: A: Condenser; B: Collector- adsorber; C: Refrigerating enclosure containing the evaporator

2.2 Measurement procedure

To analyze the effects of operating condition on the thermal behavior, the experimental setup is instrumented with (06) six type of K thermocouples placed on the various compartments of the refrigerator (glass, front and back of the absorbent plate, condenser...). The temperatures taken were those of the ambient medium (Tamb), glass cover (Tv), absorbent plate (Tp), zeolite (T), condenser (Tcd) and evaporator (Tev). These thermocouples are connected to a data logger of OBSOLETE brand (GL200A), thus, making it possible to acquire the measured data. This device leads to an accuracy of $\pm 0,5\ °C$. In addition, a KIMO solarimeter (SAM 20) is used to measure the global radiation received by the capto-adsorber. The error due to the recording with the solarimeter is $\pm 0.38\ W/m^2/°C$. All measurements were taken at intervals of fifteen (15) minutes for all the tests conducted. The various tests on the solar refrigerator took place in Yako (Burkina Faso), located between latitudes 12 ° 90 and 12 ° 96 North and between longitudes -2° 17 and -2° 26° West.

3. Numerical study

The mass and heat transfer equations in the various components (collector-adsorber, condenser, and evaporator) of the solar refrigerator were obtained from thermal balances established at each of the refrigerator components.

3.1 Assumptions

- The adsorbent is assumed to be a porous material characterized by an equivalent temperature and thermal conductivity,
- Heat transfer is unidirectional.
- The convective heat transfer and the pressure drops are neglected in the porous medium,
- The pressure is constant in the condenser and in the evaporator.

3.2 Transfer equations

The energy balance of the solar refrigerator can be divided into five regions: glass cover, absorber plate, adsorbent bed, condenser and evaporator.

The energy balance at the various components of the solar refrigerator can be written as:

$$\frac{M_i Cp_i}{S} \cdot \frac{\partial T_i}{\partial t} = \sum_{i=1}^{n} \sum_{x} \varphi_{xij} + \phi_{ch} \quad (1)$$

(φ_{xij}) is the exchanged heat flux density by the transfer mode x (conduction, convection or radiation) between media i and j (W/m^2),

(ϕ_{ch}) : heat energy during isosteric heating and desorption phase or the one of desorption and adsorption

The heat flux density (φ_{xij}) can be written as:

$$\varphi_{xij} = h_{xij}\left(T_j - T_i\right) \tag{2}$$

With h_{xij} : heat transfer by mode x between media i and j

The application of equation (1) to the components of the solar adsorption refrigerator leads to the following transfer equations:

→ ***Energy balance of glass***

$$m_v Cp_v \frac{\partial T_v}{\partial t} = \alpha_v.G_n.s_v + h_{p-v}.s_v\left(T_p - T_v\right) - h_{cv-v-ext}.s_v\left(T_v - T_{amb}\right) - h_{r-v-ciel}.s_v\left(T_v - T_{ciel}\right) \tag{3}$$

T_v is the temperature of the glass, $T_p$the temperature of the absorber plate and T_{amb} the temperature of the ambient environment.

→ ***Energy balance of absorber plate***

$$m_p Cp_p \frac{\partial T_p}{\partial t} = \left(\alpha\tau\right)_{eff} s_p G_n - h_{p-v}s_v\left(T_p - T_v\right) - h_{p-a}s_p\left(T_p - T\right) \tag{4}$$

Where T is the equilibrium temperature of the zeolite/water mixture and h_{p-a} the heat transfer coefficient between the absorber plate and this mixture.

→ ***Energy balance of adsorbent bed***

During the isosteric heating and desorption phase

$$m_{eq}Cp_{eq}\frac{\partial T}{\partial t} = h_{p-a}.s_p\left(T_p - T\right) + \delta\left(\Delta H_{des}.m_a.\frac{\partial m^{des}}{\partial t} + m_a.Cp_l\left(T - T_{cd}\right).\frac{\partial m^{des}}{\partial t}\right) \tag{5}$$

During the isosteric cooling phase and adsorption

$$m_{eq}Cp_{eq}\frac{\partial T}{\partial t} = h_{p-a}.s_p\left(T_p - T\right) + \delta\left(\Delta H_{ads}.m_a.\frac{\partial m^{ads}}{\partial t} - m_a.Cp_l\left(T - T_{ev}\right)\frac{\partial m^{ads}}{\partial t}\right) \tag{6}$$

With:

δ=0: During isosteric heating and cooling.

δ=1: During desorption and adsorption.

→ ***Condenser energy balance***

$$\left[m_{cd}.Cp_{cd} + m_d\left(t\right).Cp_l\right]\frac{\partial T_{cd}}{\partial t} = m_a.\frac{\partial m^{des}}{\partial t}\left[L_{cond}\left(P_{cd}\right) + Cp_l\left(T - T_{cd}\right)\right] - h_{r-cd-ciel}.S_{cd}\left(T_{cd} - T_{ciel}\right) - h_{cv-cd-amb}.S_{cd}\left(T_{cd} - T_{amb}\right) \tag{7}$$

Where $m_d(t)$ represents the total mass of adsorbate vapor desorbed, $T_{cd}$the temperature of the condenser and L_{cond} the latente heat of condensation.

→ ***Evaporator energy balance***

$$\left[m_{ev}Cp_{ev} + \left(m_d\left(t\right) - \Delta m.m_a\right)Cp_l\right]\frac{\partial T_{ev}}{\partial t} = -m_a\frac{\partial m^{ads}}{\partial t}\left[L_v\left(P_{ev}\right) - Cp_l\left(T - T_{ev}\right)\right] - h_{cv-ev-air}S_{ev}\left(T_{ev} - T_{air}\right) \tag{8}$$

Where T_{ev} is the temperature of the evaporator and L_v the latent heat of vaporization.

3.3 Model of adsorption kinetics

Several theories of adsorption have been proposed in the literature to describe the process of the adsorption and desorption phenomenon. The Dubinin-Astakhov equation is applied successfully to describe the adsorption of gas vapor on the adsorbent. Thus, this equation is used to calculate the rate of adsorbate (water) in the zeolite (adsorbent) as a function of temperature and pressure.

$$m = w_0\rho_l\left(T\right)\exp\left(-D\left(T\ln\frac{P_s\left(T\right)}{P}\right)^n\right) \tag{9}$$

Where $P_l(T)$ is the density of the adsorbate (water), $P_s(T)$ the saturation pressure, $W_0$the maximum adsorption capacity; D and n are constants depending on the adsorbent/adsorbate couple used. Using Antoine's equation giving the saturation pressure:

3.4 Initial conditions

For all tpt_0, t_0 being the instant from which the collector-adsorber is subjected to the solar flux, we have:

$$T_v\left(t_0\right) = T_p\left(t_0\right) = T_{ev}\left(t_0\right) = T_{cd}\left(t_0\right) = T\left(t_0\right) = T_{amb} \tag{10}$$

$$P\left(t_0\right) = P_{ev} = P_s\left(T_{ev}\right) \tag{11}$$

$$m = m(T, P) \tag{12}$$

3.5 System Performance

The solar performance coefficient (SCOP) of a solar refrigerating machine is the ratio between the amount of the cooling production to the heat input more precisely the total solar energy captured by the collector-adsorber during a day.

$$SCOP = \frac{Q_f}{\int_{t_{ar}}^{t_{ss}} A_s . G_n . dt} \tag{13}$$

Where A_s is the collecting surface and G_n is the solar irradiation

Q_f is the amount of cold product at the evaporator :

$$Q_f = m_a \Delta q \left[L(T_{ev}) - \int_{T_{ev}}^{T_{cd}} Cp_l(T)\, dT \right] \tag{14}$$

3.6 Numerical procedure

The method of solving the system of equations (3-12) which describes the transient behavior of the model is purely numerical and based on the implicit finite difference method and the Gauss Seidel iterative method. We have developed and written in Fortran a computer program to model and simulate the adsorption desorption kinetics of the zeolite/water pair and on the other hand the operation of each element of the refrigerator during a day.

3.7 Validation

To validate the numerical code, one applied it to problem of A. Allouhi et al. [34]. This problem was about a numerical study of the thermal performance of a parallelepiped-shaped collector-adsorber refrigerator with the silicagel/water as the working pair. As it is presented in figure 2, the results about the Clapeyron cycle corroborate with the one presented by A. Allouhi et al. Indeed, the maximum relative discrepancies are about 1.1% for the temperatures and 2.4% for the pressure.

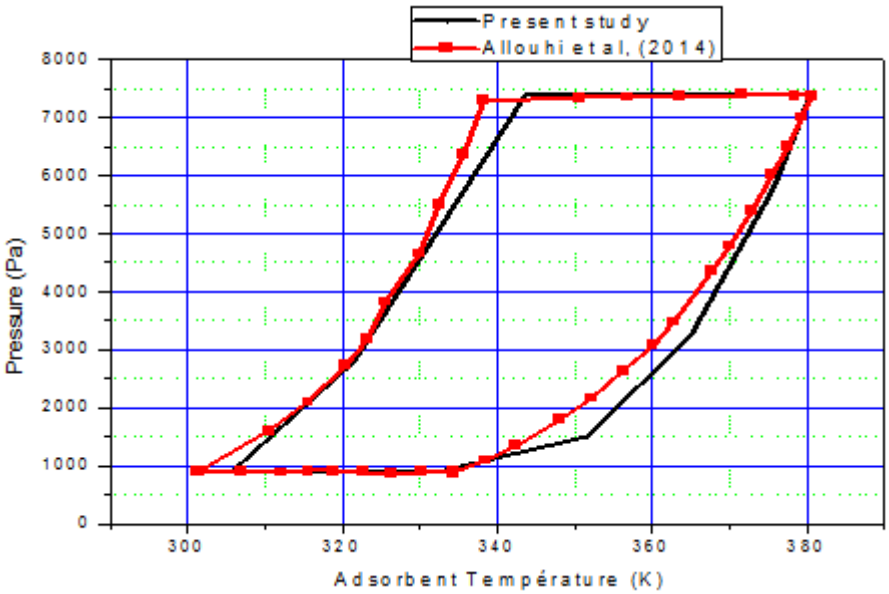

Figure 2. Clapeyron cycle

Table 1. Values of parameters used in the simulation

Symbols	Paramters	Values	Units
Properties of the adsorbent / adsorbate (zeolite/water)			
Cp_{ads}	Specific heat	0.836	[kJ.kg^{-1}.K^{-1}]
ρ_{ads}	Density	620	[kg.m^{-2}]
Cp_l	Specific heat	4.18	[kJ.kg^{-1}.K^{-1}]
Collector-adsorber			
ε_v	Emissivity of the glass	0.9	[-]
τ_v	Transmitivity of the glass	0.95	[-]
α_v	Absorptivity of the glass	0.05	[-]
e_v	Thickness of the glass	0.04	[m]
S	Area	1	[m^2]
Cp_v	Specific heat of the glass	0.75	[kJ.kg^{-1}.K^{-1}]
Cp_p	Specific heat of the absorbent plate	0.896	[kJ.kg^{-1}.K^{-1}]
e_p	Thickness of absorbent plate	0.05	[m]
α_p	Absorptivity of absorbent plate	0.95	[-]
ε_p	Emissivity of the absorbent plate	0.9	[-]
Parameters of Dubinin- Astakhov			
D	Characteristic parameter of the adsorbent / adsorbate couple	4.15 10^{-7}	[-]
N	Characteristic parameter of the adsorbent / adsorbate couple	2	[-]
W_o	Maximum adsorption capacity	0.269 10^{-3}	[m^3.kg^{-1}]

4. Results and Discusions

4.1 Dynamic behavior

Figure 3 shows hourly the evolution of global solar irradiation and the one of the ambient temperature during a day. As presented in this figure, the global solar irradiation and the ambient temperature increase during the morning until a maximum value of 824 W/m^2 at 13h and 30°C at 16h. It can be noted that the ambient temperature decreases in the afternoon until (25°C). A value that remains important even in the absence of the solar irradiation. These values thus obtained (figure 3) and the values in Table 1 were used for the simulation of our model.

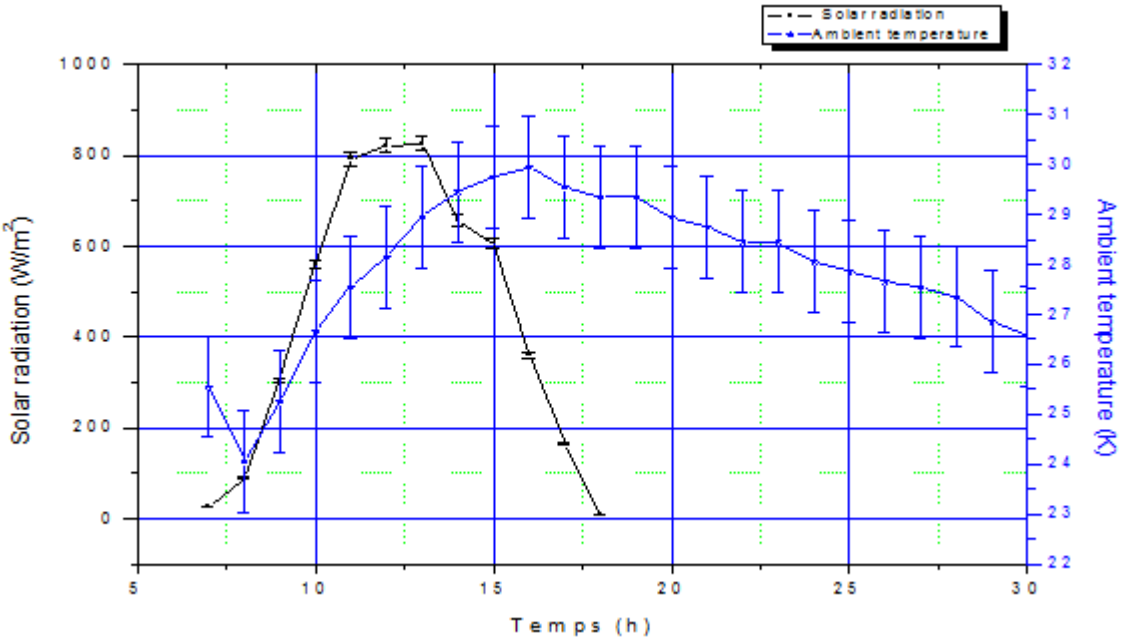

Figure 3. Hourly evolution of solar radiation and ambient temperature

Figure. 4 shows the comparative evolution of the simulated and experimental temperatures of the various components of the solar adsorption refrigerator. This comparison is focused on the temperature of the absorbent plate, the adsorbent bed (zeolite), the condenser and the evaporator. Indeed, the comparison of the results obtained from the two models (numerical model and experimental model) allows us to say that the numerical model qualitatively represents the functioning of the solar refrigerator. This can be explained by the fact that the experimental and simulated data obtained have the same characteristics. However, errors were observed at the quantitative level.

The differences between the simulated and experimental temperature curves of the absorbent plate and the zeolite are higher in the middle of the day than at the end of the day. This is justified by the low density of the solar flux received by the collector-adsorber due to the shadow of the building. In addition, the experimental temperature of the zeolite was evaluated by averaging between the temperature of the front and back face of the adsorber. We do not introduce a thermocouple inside the adsorber for the sake of sealing. This is the reason for this difference between the measured and simulated data.

Concerning the condenser, the experimental and simulated curves agree mainly for the first hours of the day. Beyond the noon, the difference between these curves becomes more and more important and the experimental values are higher. These significant differences observed between the simulated and experimental temperatures in the afternoon are justified by the low air velocity and the heat of the radiation of the walls of the chamber in which the condenser is located, as this additional load was not taken into account in the modeling.

The difference between the simulated and experimental temperatures at the evaporator level is important at the beginning of the day but decreases significantly at the end of the day. This difference is due to the presence of water in the experimental prototype to serve as cold storage produced the previous day.

Table 2 presents a comparison of the amount of cold produced, the amount of heat received and the SCOP obtained by simulation and experimentation. There is a relative difference between the experimental results and those obtained by the simulation. Nevertheless, since the experimental conditions are not strictly those used in our calculation code, we can say that the simulated and experimental results reveal a good agreement.

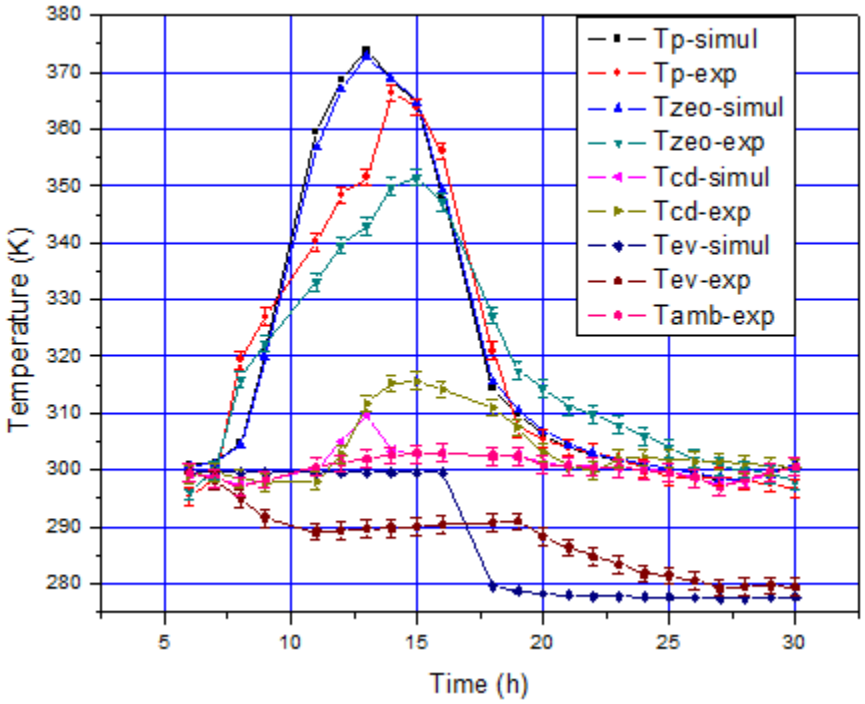

Figure 4. Hourly evolution of the simulated and experimental temperatures of the various components of the solar refrigerator

Table 2. Coefficient of performance of the solar adsorption refrigerator

	Experimental results				**Numerical results**	
	05/8/2016	04/8/2016	14/12/2016	15/12/2016	August (05/8/2016)	December (15/12/2016)
Qf [MJ]	1,89	2,219	3,366	3,459	2,1098	4,642
Qc [MJ]	18,15	21,86	19,972	18,589	18,63	22.02
SCOP	0,103	0,101	0,168	0,186	0,113	0,21

The hourly evolution of the pressure in the adsorbent bed and the mass of adsorbed adsorbate are shown in figure 5. During the day, the pressure increases until reaching the saturation pressure corresponding to the condensation temperature (P = Pcd = 7376 Pa) and remains constant during 5 hours. This pressure decreases as the temperature of the adsorbent bed decreases until the evaporation pressure (P = Pev = 872 Pa) and stays constant during the evaporation-adsorption phase (12 hours).

During the cycle, the quantity of water adsorbed in the adsorbent bed (zeolite) decreases during the desorption phase, then increases during the adsorption phase. It remains constant during the isosteric heating and cooling phases. These results correspond with those previous works such as, [12, 15, 34].

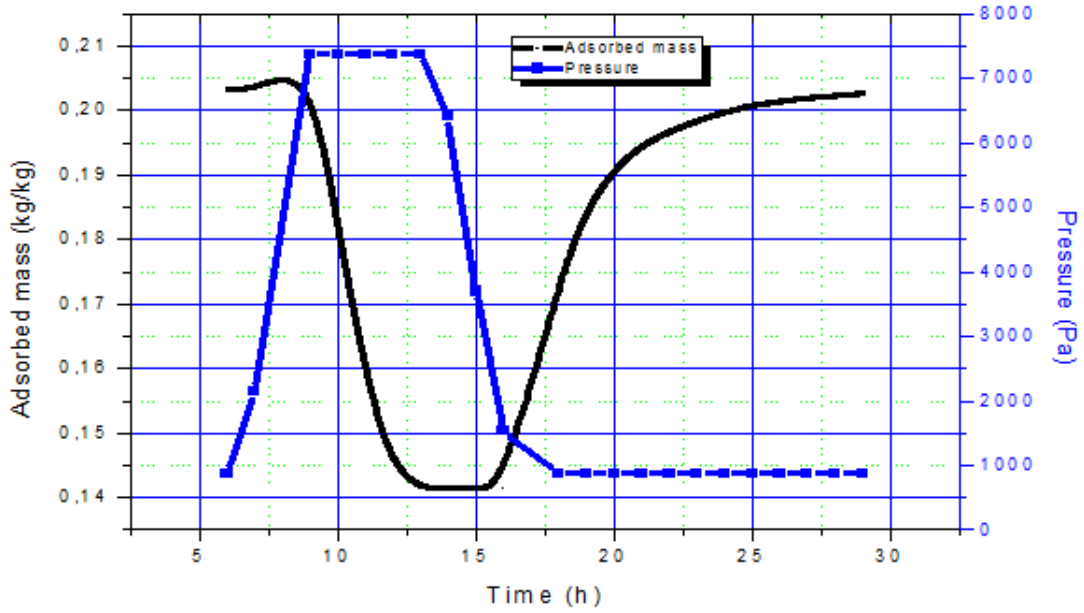

Figure 5. Evolution of the pressure and the adsorbed mass

4.2 Parametric study

4.2.1 Influence of climatic conditions

The data (ambient temperature and solar radiation) are important parameters that affect the performance of adsorption solar refrigerator systems. For that, the values of these two (02) parameters of each month of the year were introduced into our calculation code in order to predict the behavior of the system throughout the year. The average meteorological data were provided by the General Direction of Meteorology of Burkina Faso for the period 1992-2006. The monthly SCOP calculated by a dynamic simulation and the average meteorological data is presented in Figure 6. It can be noted that in this figure the SCOP varies between 0.11 and 0.25 during the year. The lowest value of the SCOP is obtained on August and the largest on March. Indeed, on August, the solar energy received by the collector-adsorber is low. This is due to the cloudy sky and to the sudden weather variations related to rain events. This solar energy is insufficient to allow a good desorption of the water vapor; it is therefore mainly used for heating the components of the collector-adsorber. During March, the desorption of the water vapor is optimal due to the strong sunshine, and to the state of the sky which is clear.

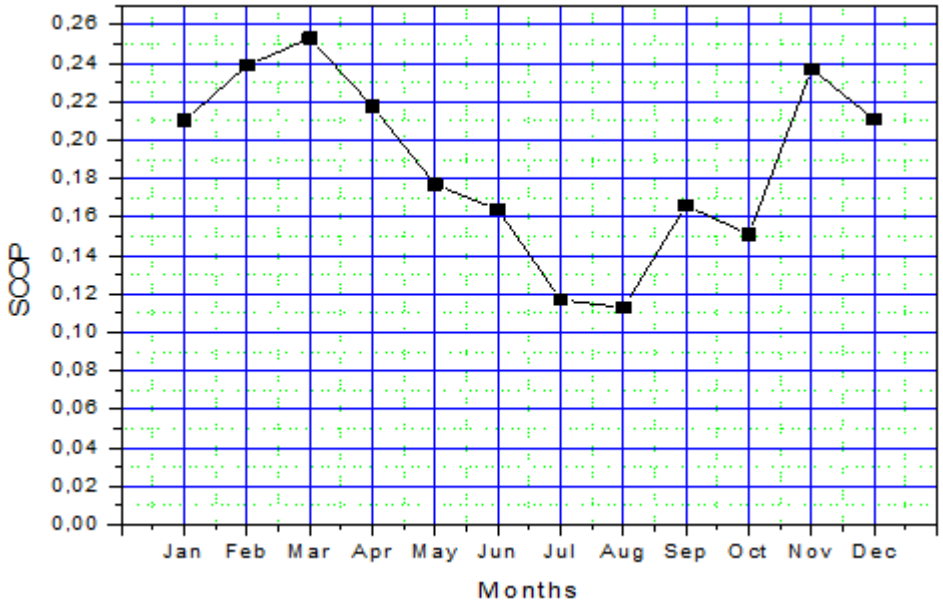

Figure 6. SCOP simulated during the 12 months of the year

4.2.2 Influence of evaporator temperature

Figure 7 illustrates the effect of the increase of the temperature of the evaporator on the amount of cold produced in the evaporator (Qf) and the SCOP. One can note that an increase of the temperature of the evaporator from 275 to 287 K, provokes an augmentation of the amount of cold produces (Qf) and of the SCOP. Indeed, the temperature of the evaporator controls the adsorption process which begins when the pressure in the adsorber has the same value as that of the evaporator. Hence, the increase in the evaporation temperature leads to an increase in the saturation pressure at this temperature (Ps (Tev)). In addition, the adsorbed mass of water vapor (Ta, Ps (Tev)) increases in the cycle. Consequently, the amount of cold produced (Qf) and the SCOP of the system increases as the evaporation temperature increases. These results correspond to previous studies such as A. Almers et al., Konfe, A et al., A. Allouhi et al., H. Hassan [13, 35, 36, 37].

4.2.3 Influence of condenser temperature

Figure 8 shows the effect of the temperature of the condenser on the amount of cold produced (Qf) and on the SCOP. As it can be seen in this figure, the amount of cold produced (Qf) and the SCOP decreases with increasing of the condenser temperature. Indeed, the increase of the condenser temperature causes an increase of the desorption pressure as well as that of the desorption threshold temperature. This results in a decrease in the cyclic mass and therefore a decrease in Qf and SCOP. The result is in agreement with the one reported by A. Almers et al., [35] in a numerical study carried out on a minus-fin tube collector-adsorber using activated carbon / ammonia in order to optimize the dimensioning of this refrigeration system. In addition, it is also in agreement with those of A. Allouhi et al., W. Chekirou et al., [34, 38].

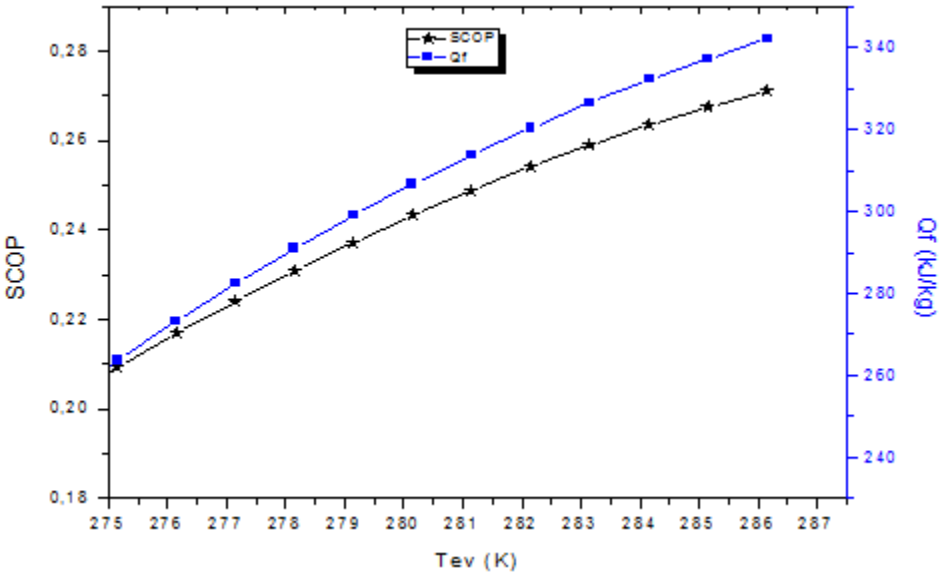

Figure 7. Influence of evaporator temperature on SCOP and Qf

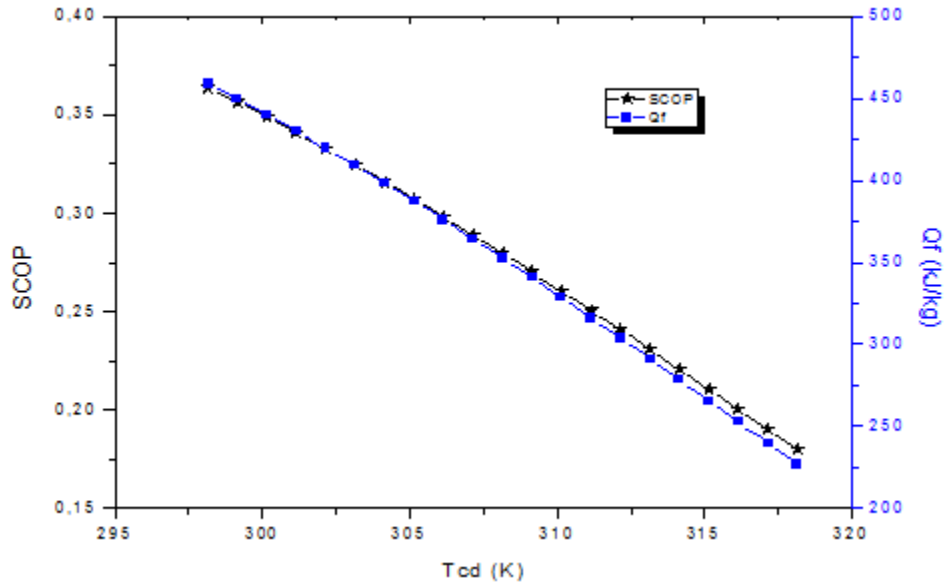

Figure 8. Influence of condenser temperature on SCOP and Qf

5. Conclusion

A numerical and experimental study of the operation of a solar adsorption refrigerator using the zeolite-water pair is presented. Transfer equations, based on thermal balance established on each component of the solar adsorption refrigerator associated to the Dubinin-Astakhov equation are solved using an implicit numerical scheme and Gauss iterative method. The experimental part is focused on the measurement of the temperature of the component of a prototype solar adsorption refrigerator operating in Yako (Burkina Faso). Results are presented by the amount of cold produced, the SCOP and the hourly evolution during a day of the temperature of the components of the solar adsorption refrigerator.

From the analysis performed above, some conclusions are summarized as follows:

• Numerical results corroborate with experimental data.

• Temperatures of condenser and evaporator have major effects on the solar performance coefficient

• The weather conditions have major influence on its performance. During the months of March and August, the average solar flux densities are 590 W/m2 and 436 W/m2 respectively. The amount of cold produced during these months is 6.391 MJ for the month of March and 2.12 MJ for the month of August. This gives a SCOP of 0.25 and 0.11 for the months of March and August.

References

[1] E. Anyanwu, «Environmental pollution: restructuring the refrigeration industry as a way out.,» *Environment Protection Engineering*, pp. 26(4);17-28, 2000.

[2] M. Hadj Ammara, B. Benhaoua et M. Balghouthi, «Simulation of tubular adsorber for adsorption refrigeration system powered by solar energy in sub-Sahara region of Algeria,» *Energy Conversion and Management* , p. 106 (2015) 31–40, 2015.

[3] M. Umair, A. Akisawa et Y. Ueda, «Performance evaluation of a solar adsorption refrigeration system with a wing type compound parabolic concentrator.,» *Energies*, pp. 7,1448–1466., 2014.

[4] D. Wang, J. Zhang, Q. Yang, N. Li et K. Sumathy, «Study of adsorption characteristics in silica gel–water adsorption refrigeration.,» *Appl. Energy*, pp. 113, 734–741, 2014.

[5] N. Qasem et M. El-Shaarawi, «Improving ice productivity and performance for an activated carbon/methanol solar adsorption ice-maker.,» *Sol. Energy*, pp. 98, 523–542, 2013.
[6] Z. Lu, R. Wang, Z. Xia et L. Gong, « Experimental investigation adsorption chillers using micro-porous silica gel-water and compound adsorbent-methanol.,» *Energy Convers. Manag*, pp. 65, 430–437, 2013.
[7] K. Habib, B. Choudhury, P. Chatterjee et B. Saha, «Study on a solar heat driven dual-mode adsorption chiller,» *Energy*, pp. 63, 133–141, 2013.
[8] A. Chikouche, «Using solar energy for refrigeration purposes in Algeria,» *chez 4th JIIRCRAC Proceeding*, 2012.
[9] Marlinda, A. Uyun, T. Miyazaki, Y. Ueda et A. Akisawa, « Performance analysis of a double-effect adsorption refrigeration cycle with a silica gel/water working pair,» *Energies*, pp. 3,1704–1720., 2010.
[10] D. Wang et J. Zhang, « Design and performance prediction of an adsorption heat pump with multi-cooling tubes,» *Energy Convers. Manag*. , pp. 50, 1157–1162., 2009.
[11] A. Rahman, Y. Ueda, Y. Akisawa, T. Miyazaki et B. Saha, «Design and performance of an innovative four-bed, three-stage adsorption cycle,» *Energies*, pp. 6, 1365–1384, 2003.
[12] H. Hassan, A. Mohamad et R. Bennacer, «Simulation of an adsorption solar cooling system.,» *Energy* , pp. 36, 530–537., 2011.
[13] H. Hassan, «Energy analysis and performance evaluation of the adsorption refrigeration system.,» *ISRN Mech. Eng*, pp. 2013, 704340, 2013.
[14] H. Hassan, A. Mohamad et H. Al-Ansary, «Development of a continuously operating solar-driven adsorption cooling system: Thermodynamic analysis and parametric study,» *Appl. Therm. Eng*, pp. 48, 332–341, 2012.
[15] M. Louajari, A. Mimet et A. Ouammi, «Study of the effect of finned tube adsorber on theperformance of solar driven adsorption cooling machine using activated carbon-ammonia pair.,» *Appl. Energy* , pp. 88, 690–698., 2011.
[16] M. Ousmane, B. Dianda, S. Kam, A. Konfe, T. Ky et D. Bathiebo, « Experimental study in natural convection.,» *Global Journal of Pure and Applied Sciences*. , p. 21(2):155., 2015.
[17] A. E. Fadar, «Thermal behavior and performance assessment of a solar adsorptioncooling system with finned adsorber ;,» *Energy* , pp. 83 (2015) 674-684, 2015.
[18] R. E. Critoph, Carbon Materials for advanced technologies, adsorption refrigerators and heat pumps, chapter 10,, USA: Edited by Timonthy D. Burchell,, 1999.
[19] A. Mhimid, A. A. Jemni et B. Nasrallah.S., «Etude théorique des transferts couples de chaleur et de masse lors de la désorption du couple Zéolithe 13X- eau.,» *Rev. Gen. Ther*, pp. 36, pp 697-706, 1997.
[20] A. Jemni et S. Ben Nasrallah, « Study of two-dimensional heat and mass transfer during desorption in a metal- hydrogen reactor.,» *Int. J. Hydrogen Energy*, , pp. Vol. 20, pp 881- 891, 1995.
[21] R. Critoph et L. Turner, «Heat transfer in granular activated carbon beds in the presence of adsorbable gases.,» *Int. J. Heat Tran*, pp. 38 (9), 1577-1585, 1995.
[22] A. Almers, A. Azzabakh et A. Mimet, «Optimal design study of cylindrical finned reactor for solar adsorption cooling machine working with activated carbon-ammonia pair,» *Applied thermal engineering*, pp. 26, 1866 - 1875, 2006.
[23] F. Meunier, «Adsorptive cooling: a clean technology,» *Clean Prod. Proc*. , n° %13, 8-20., 2001.
[24] E. Anyanwu, «Review of solid adsorption solar refrigerator I: an overview of the refrigeration cycle.,» *Energ. Conv. Mgn*. , pp. 44, 301-312, 2003.
[25] W. Chekirou, W. Boukheit et T. Kerbache, «Numerical modeling of combined heat and mass transfer in a tubular adsorber of a solid adsorption solar refrigerator.,» *Revue des Energies Renouvelables* , pp. 10 (3), 367–379, 2007.
[26] A. Naef, M. A. Qasem et El-Shaarawi, « Improving ice productivity and performance for an activated carbon/methanol solar adsorption ice-maker ;,» *Solar Energy* , p. 98 (2013) 523–542, 2013.
[27] M. Li, C. Sun, R. Wang et W. Cai, « Development of no valve solar ice maker.,» *Appl Therm Eng* , pp. 24(5-6):865–72., 2004.
[28] A. Leite, M. Grilo, R. Andrade, F. Belo et F. Meunier, « Experimental thermodynamic cycles and performance analysis of a solar-powered adsorptive ice maker in hot humid climate.,» *Energy Renewable* , pp. 32, 697–712., 2007.
[29] U. Muhammad, A. Atsushi et U. Yuki, « Performance Evaluation of a Solar Adsorption Refrigeration System with a Wing Type Compound Parabolic Concentrator,» *Energies* , pp. 7, 1448-1466; , 2014.
[30] M. Bakkas, M. Mada et M. Tahri, «Modélisation et Simulation du Transfert de Chaleur et de Masse à l'Intérieur d'un Réacteur de Charbon Actif Réagissant avec de l'Ammoniac Couplé à un Caloduc Annulaire à Eau ;,» *Rev. Energ. Ren. : Journées de Thermique*, pp. (2001) 19-24, 2001.
[31] A. Allouhi, T. Kousksou, A. Jamil, T. El Rhafiki, Y. Mourad et Y. Zeraouli, «Optimal working pairs for solar adsorption cooling applications.,» *Energy*. , p. 79:235–247., 2015.
[32] A. D. M. Leite, « Performance of a new solid adsorption ice maker with solar energy regeneration. Energ.,» *Conv. Mgn*., pp. 41, 1625-1647, 2000.
[33] J. M. F. Guilleminot, « Heat and mass transfer in a non isothermal fixed bed solid adsorbent reactor a uniform pressure-non uniform temperature.,» *Int. J. Heat. Mass. Trans*., pp. 30 (8), 1595-1606., 1987.
[34] A. Allouhi, T. Kousksou, A. Jamil et Y. Zeraouli, «Modeling of a thermal adsorber powered by solar energy for refrigeration applications,» *Energy*, n° %175, pp. 589-596, 2014.
[35] A. M. A. Al Mers, « Numerical study of heat and mass transfer in adsorption porous medium heated by solar energy: Boubnov-Galerkin method,» *Heat Mass Trans*, pp. 41,717-723., 2005.
[36] A. Konfe, S. Kam, M. Ousmane et D. J. Bathiebo, «Comparative Thermodynamic Study of Five Couples Used in Solar Cooling with Adsorption by Simulation,» *British Journal of Applied Science & Technology*, pp. 17(2): 1-17, 2016.

[37] A. Allouhi, T. Kousksou, A. Jamil, Y. Agrouaz, T. Bouhal, R. Saidur et A. Benbassou, «Performance evaluation of solar adsorption cooling systems for vaccine preservation in Sub-Saharan Africa,» *Applied Energy*, pp. 170, 232–241, 2016.
[38] W.Chekirou, R. Boussehain, M. Feidt , A. Karaali, N. Boukheit, «Numerical Results on Operating Parameters Influence for a Heat Recovery Adsorption Machine» *Energy Procedia*, 6 (2011) 202–216.

Nomenclature

Cp	Spécific heat (J/kg.K)	ΔH	Heat of adsorption/desorption (J/kg)
D	Constant in the Dubinin-Astakhov equation	**Subscripts**	
Gn	Solar radiation (W/m^2)	a	adsorption
m	mass (kg)	ads	adsorbent
n	Constant in the Dubinin-Astakhov equation	d	desorption
P	Pressure (Pa)	cd	condenser
P_s	Saturation Pressure (Pa)	ev	evaporator
Q_f	Cold production (J)	v	glass
q	Water concentration inside the zéolithe (kg/kg)	ext	outside
S	Area (m^2)	amb	ambient
T	Température (K)	zeo	zeolithe
t	Time (s)	min/max	minimum
W_o	Parameter of Dubinin-Astrakhov equation (m^3/kg)	max	maximum
L(T)	Latent heat of vaporization (J/kg)	g	generation
Greek Letters :		cv	convection
α	absorptance	moy	average
τ	Transmitance	wa	water
Δt	Time step (s)		